

 <p>ISSN NO. 2320-5407</p>	<p>Journal Homepage: - www.journalijar.com</p> <p>INTERNATIONAL JOURNAL OF ADVANCED RESEARCH (IJAR)</p> <p>Article DOI: 10.21474/IJAR01/1508 DOI URL: http://dx.doi.org/10.21474/IJAR01/1508</p>	 <p>INTERNATIONAL JOURNAL OF ADVANCED RESEARCH (IJAR) ISSN 2320-5407</p> <p>Journal homepage: http://www.journalijar.com Journal DOI: 10.21474/IJAR01</p>
---	---	---

RESEARCH ARTICLE

GENERATION OF WHISTLER MODE WAVES BY INJECTION OF COLD ELECTRON BEAM FOR LOSS-CONE DISTRIBUTION WITH AC ELECTRIC FIELD IN MAGNETO-PLASMA.

R.S. Pandey¹, Rajbir Kaur^{1*}, Vineeta Kumari² and K.M. Singh².

1. Department of Physics, Amity Institute of Applied Sciences, Amity University, Sector 125, Noida, Uttar Pradesh – 201313, India.
2. Department of Physics, VKS University, Ara, Bihar-802301.

Manuscript Info

Manuscript History

Received: 15 July 2016
Final Accepted: 16 August 2016
Published: September 2016

Key words:-

Whistler mode waves, Loss cone distribution function, Magnetosphere.

Abstract

Parallel propagating whistler mode waves, in the presence of AC electric field perpendicular to the ambient magnetic field has been studied for magneto-plasma under the effect of beam injection. The dispersion relation and growth rate have been derived and calculations are performed for pitch angle loss cone unperturbed distribution function. The present analysis shows that the growth rate of whistler mode wave has been found to be varying with the values of temperature anisotropy, number density of injected beam and loss cone angle. It is also inferred that even in the absence of temperature anisotropy, there is growth of whistler waves, implying dominant role played by loss-cone angle in generating whistler mode instability.

Copy Right, IJAR, 2016,. All rights reserved.

Introduction:-

In plasma the charged particles respond very well to electrostatic and electromagnetic fields. The fields could be oscillatory or static. Strong interactions occur between charged particles and plasma waves leading to instabilities. The study of these plasma waves and instabilities is important in understanding and explaining the state of plasma, plasma flux in magnetized plasma, evolution of energy and plenty of more interesting phenomena. When plasma waves propagate, they are strongly influenced by magnetized plasma.

Whistlers are low frequency, circularly polarized electromagnetic waves in the audio-frequency range. Wave particle interaction can also create whistler mode radiations in the magnetosphere. Whistler mode emission constitutes electromagnetic waves with frequency below either electron gyro frequency or local electron plasma frequency, whatever is less. Calculation shows that either a loss-cone or a thermal anisotropy in the hot plasma component of the magnetosphere can lead to the generation of incoherent emission of low frequency whistler waves (Pandey and Singh, 2010). Coherent, oblique whistler chorus elements may provide the scattering mechanism that drives the precipitation. Two types of electron trapping by whistlers can be studied in literature. First one is trapping of electrons at a fixed phase of the whistler in a cyclotron resonance. In this case electrons are considered moving through the whistler, and then encounter an electric field that rotates in synchronism with the velocity of electron (Matsumoto and Omura, 1981; Omura and Matsumoto, 1982). The second one, is trapping in the electrostatic potential of an oblique whistler (Kumagai et al. 1980).

A substantial increase in the energetic electron precipitation was found by the injection of very modest amount of cold plasma into the radiation belt of magnetosphere (Brice and Lucas, 1971). Since then, because of the possibility

Corresponding Author:- Rajbir Kaur.

Address:- Department of Physics, Amity Institute of Applied Sciences, Amity University, Sector 125, Noida, Uttar Pradesh – 201313, India.

of excitation of specific modes in magnetosphere, more investigations have been done in whistler mode instability. Parallel propagating plasma waves in the vicinity of magnetosphere at very low frequencies have been studied by many workers. Using a series of 1-d simulations, the growth of whistler wave was studied by Zhang et al. (1993) from an anisotropic electron beam of various electrostatic and electromagnetic wave modes at various propagation angles. The charged particles in ionosphere and magnetosphere exhibit anisotropic distribution in momentum space, which is suitable for cyclotron instability. This leads to growth in wave, so particle precipitate into the atmosphere. Singh et al. (2006) evaluated the effect of thermal velocity of plasma particles on the energy of resonantly interacting energetic electrons with the propagating whistler mode waves as a function of wave frequency and L-value for the normal and disturbed magnetospheric conditions. Bret et al. (2006) systematically worked the electromagnetic instabilities in the whole k space for a cold relativistic beam interacting with transversely hot plasma.

The acceleration and scattering of particles, the damping or the growth of waves and the emission of radiations are the consequences of wave-particle interaction. The interactions in which wave exchanges energy with the particles, play crucial role in several phenomena occurring in space plasma (Gary, 1992) and in laboratory (Gill, 1981). Resonant wave-particle interactions are a basic problem, particularly in magnetospheric physics. Since low frequency waves interact with charged particles over long scale lengths within magnetospheres and can transfer energy from one region to another, we chose to study these low frequency whistler mode waves in an inhomogeneous magnetosphere.

Being inspired from above findings, in this paper whistler mode instability with field lines propagation for loss cone unperturbed distribution function in presence of injected beam are analyzed for magneto-plasma. In present study, we have investigated the wave-particle interaction taking place between the whistler mode waves in the magnetosphere and energetic electrons trapped in the radiation belts of the magnetosphere. The magnetic field considered is the magnetic field of Earth, thus called the external magnetic field, assumed constant. And the time varying electric field considered, is the field generated by the particles oscillating along the magnetic field lines of the planet. AC electric field perpendicular to the ambient magnetic field is studied. The dispersion relation in growth rate have been derived and calculated for magneto-plasma. Parametric studies are performed by changing plasma parameters: temperature anisotropy, AC frequency, thermal velocity and loss-cone angle.

Dispersion Relation:-

A spatially homogeneous an isotropic, collision less magneto plasma subjected to an external magnetic field $\mathbf{B}_0 = B_0 \hat{\mathbf{e}}_z$ and electric field $\mathbf{E}_0 = (E_0 \sin \nu t \hat{\mathbf{e}}_x)$ has been considered in order to obtain the relation. In case, the Vlasov-Maxwell equations are linearized. The linearized equations obtained after neglecting the higher order terms and separating the equilibrium and non- equilibrium parts, following the techniques of Pandey and Singh (2012) are given as

$$\mathbf{v} \cdot \frac{\partial f_{s0}}{\partial \mathbf{r}} + \frac{e_s}{m_s} [\mathbf{E}_0 \sin \nu t + (\mathbf{v} \times \mathbf{B}_0)] \left(\frac{\partial f_{s0}}{\partial \mathbf{v}} \right) = 0 \quad \dots(1)$$

$$\frac{\partial f_{s1}}{\partial t} + \mathbf{v} \cdot \frac{\partial f_{s1}}{\partial \mathbf{r}} + \left(\frac{\mathbf{F}}{m_s} \right) \left(\frac{\partial f_{s1}}{\partial \mathbf{v}} \right) = S(\mathbf{r}, \mathbf{v}, t) \quad \dots(2)$$

Where force is defined as $\mathbf{F} = m \, d\mathbf{v}/dt$

$$\mathbf{F} = e_s [\mathbf{E}_0 \sin(\nu t) + (\mathbf{v} \times \mathbf{B}_0)] \quad \dots(3)$$

The particle trajectories are obtained by solving equation of motion defined in equation (3) and $S(\mathbf{r}, \mathbf{v}, t)$ is defined as:

$$S(\mathbf{r}, \mathbf{v}, t) = (e/m_s) [E_1 + (\mathbf{v} \times \mathbf{B}_1)] \left(\frac{\partial f_{s0}}{\partial \mathbf{v}} \right) \quad \dots(4)$$

where s denotes species and E_1 , B_1 and f_{s1} are perturbed quantities and are assumed to have harmonic dependence in E_1 , B_1 and $f_{s1} = \exp i(\mathbf{k} \cdot \mathbf{r} - \omega t)$.

The method of characteristic solution is used to determine the perturbed distribution function, f_{s1} , which is obtained from Eq. (2) by

$$f_{s1}(\mathbf{r}, \mathbf{v}, t) = \int_0^\infty S\{\mathbf{r}_0(\mathbf{r}, \mathbf{v}, t'), \mathbf{v}_0(\mathbf{r}, \mathbf{v}, t'), t - t'\} dt'$$

The phase space coordinate system has been transformed from $(\mathbf{r}, \mathbf{v}, t)$ to $(\mathbf{r}_0, \mathbf{v}_0, t - t')$. The particle trajectories which are obtained by solving eq. (3) for the given external field and wave propagation, $\mathbf{k} = [k_\perp \hat{e}_x, 0, k_\parallel \hat{e}_z]$ are:

$$\begin{aligned} \mathbf{x}_0(0) &= \mathbf{x}(t) + \left(\frac{\mathbf{v}_y(t)}{\omega_{cs}} \right) + \left(\frac{1}{\omega_{cs}} \right) \left[\{ \mathbf{v}_x(t) \} \sin \omega_{cs} t' - \{ \mathbf{v}_y(t) \} \cos \omega_{cs} t' \right] + \left(\frac{\Gamma_x}{\omega_{cs}} \right) \left[\frac{\omega_{cs} \sin \omega_{cs} t' - v \sin \omega_{cs} t'}{\omega_{cs}^2 - v^2} \right] \\ \mathbf{y}_0(0) &= \mathbf{y}(t) + \left(\frac{\mathbf{v}_x(t)}{\omega_{cs}} \right) - \left(\frac{1}{\omega_{cs}} \right) \left[\{ \mathbf{v}_x(t) \} \cos \omega_{cs} t' - \{ \mathbf{v}_y(t) \} \sin \omega_{cs} t' \right] - \left(\frac{\Gamma_x}{\omega_{cs}} \right) \left[1 + \frac{v^2 \cos \omega_{cs} t' - \omega_{cs}^2 \cos \omega_{cs} t'}{\omega_{cs}^2 - v^2} \right] \\ \mathbf{z}_0(0) &= \mathbf{z}(t) - \{ \mathbf{v}_z(t) \} t' \end{aligned} \quad \dots(5)$$

and the velocities are

$$\begin{aligned} \mathbf{v}_{x0}(0) &= \{ \mathbf{v}_x(t) \} \cos \omega_{cs} t' - \{ \mathbf{v}_y(t) \} \sin \omega_{cs} t' + \left\{ \frac{v \Gamma_x (\cos \omega_{cs} t' - \cos \omega_{cs} t')}{\omega_{cs}^2 - v^2} \right\} \\ \mathbf{v}_{y0}(0) &= \{ \mathbf{v}_x(t) \} \sin \omega_{cs} t' + \{ \mathbf{v}_y(t) \} \cos \omega_{cs} t' - \left\{ \frac{\Gamma_x (\omega_{cs} \sin \omega_{cs} t' - v \sin \omega_{cs} t')}{\omega_{cs}^2 - v^2} \right\} \\ \mathbf{v}_{z0}(0) &= \mathbf{v}_z(t) \end{aligned} \quad \dots(6)$$

where $\omega_{cs} = \frac{e_s B_0}{m_s}$ is the cyclotron frequency of species s and $\Gamma_x = \frac{e_s E_0}{m_s}$ and AC electric field is varying as $E = E_{0x} \sin \omega_{cs} t$, v being the angular AC frequency.

After doing some lengthy algebraic simplification and carrying out the integration, the perturbed distribution function f_1 is written as Pandey et al [2010].

$$\begin{aligned} f_{s1}(\mathbf{r}, \mathbf{v}, t) &= -\frac{e_s}{m_s \omega_{m,n,p,q}} \sum_{\mathbf{k}} \frac{J_p(\lambda_2) J_m(\lambda_1) J_q(\lambda_3) e^{i(\mathbf{k} \cdot \mathbf{r} - \omega t)}}{(\omega - \mathbf{k}_\parallel \mathbf{v}_\parallel - (n+q)\omega_{cs} + p v)} \left[E_{1x} J_n J_p \left\{ \left(\frac{n}{\lambda_1} \right) U^* + D_1 \left(\frac{p}{\lambda_2} \right) \right\} \right] \times \\ &\quad - i E_{1y} \{ J'_n J_p C_1 + J_n J'_p D_2 \} + E_{1x} J_n J_p W^* \dots(7) \end{aligned}$$

where the Bessel identity

$$e^{i\lambda \sin \theta} = \sum_{k=-\infty}^{\infty} J_k(\lambda) e^{ik\theta}$$

has been used, the arguments of the Bessel functions are

$$\lambda_1 = \frac{\mathbf{k}_\perp \mathbf{v}_\perp}{\omega_{cs}}, \quad \lambda_2 = \frac{\mathbf{k}_\perp \Gamma_x v}{\omega_{cs}^2 - v^2}, \quad \lambda_3 = \frac{\mathbf{k}_\perp \Gamma_x v}{\omega_{cs}^2 - v^2} \quad \dots(8a)$$

$$C_1 = \frac{1}{\mathbf{v}_\perp} \left(\frac{\delta f_o}{\delta \mathbf{v}_\perp} \right) (\omega - \mathbf{k}_\parallel \mathbf{v}_\parallel) + \left(\frac{\delta f_o}{\delta \mathbf{v}_\parallel} \right) \mathbf{k}_\parallel \quad \dots(8b)$$

$$U^* = C_1 \left[\mathbf{v}_\perp - \left(\frac{v \Gamma_x}{\omega_{cs}^2 - v^2} \right) \right] \quad \dots(8c)$$

$$\begin{aligned} W^* &= \left[\left(n \omega_{cs} \frac{\mathbf{v}_\parallel}{\mathbf{v}_\perp} \right) \left(\frac{\delta f_o}{\delta \mathbf{v}_\perp} \right) - n \omega_{cs} \left(\frac{\delta f_o}{\delta \mathbf{v}_\perp} \right) \right] + \\ &\quad + \left[1 + \left\{ \frac{\mathbf{k}_\perp \Gamma_x v}{\omega_{cs}^2 - v^2} \right\} \right] \left\{ \frac{p}{\lambda_2} - \frac{n}{\lambda_1} \right\} \end{aligned} \quad \dots(8d)$$

$$D_1 = C_1 \left(\frac{v \Gamma_x}{\omega_{cs}^2 - v^2} \right), \quad D_2 = C_2 \left(\frac{\omega_{cs} \Gamma_x}{\omega_{cs}^2 - v^2} \right) \quad \dots(8e)$$

$$J'_n = \frac{dJ_n(\lambda_1)}{d\lambda_1}, J'_p = \frac{dJ_p(\lambda_2)}{d\lambda_2} \quad \dots(8f)$$

The conductivity tensor $\|\sigma\|$ is written as

$$\|\sigma\| = -\sum \frac{e_s^2}{m_s \omega} \sum_{m,n,p,q} \int \frac{J_q(\lambda_3) S_{ij} d^3 v}{\omega - \mathbf{k}_{\parallel} \mathbf{v}_{\parallel} - (n+q)\omega_{cs} + p\nu} \dots (9)$$

where

$$\|\mathbf{S}\| = \begin{vmatrix} \mathbf{v}_{\perp} J_n^2 J_p \left(\frac{n}{\lambda_1}\right) A & i \mathbf{v}_{\perp} J_n B & \mathbf{v}_{\perp} J_n^2 J_p \left(\frac{n}{\lambda_1}\right) W^* \\ \mathbf{v}_{\perp} J_n' J_n J_p A & \mathbf{v}_{\perp} J_n' B & i \mathbf{v}_{\perp} J_n' J_n J_p W^* \\ \mathbf{v}_{\parallel} J_n^2 J_p A & \mathbf{v}_{\parallel} J_n B & \mathbf{v}_{\parallel} J_n^2 J_p W^* \end{vmatrix} \dots (10)$$

$$A = \left(\frac{n}{\lambda_1}\right) U^* + \left(\frac{p}{\lambda_2}\right) D_1, \quad B = J_n' J_p C_1 + J_n' J_n D_2$$

From $\mathbf{J} = \|\sigma\| \mathbf{E}_1$ and two Maxwell's curl equations for the perturbed quantities, we have

$$\left[\mathbf{k}^2 - \mathbf{k} \cdot \mathbf{k} - \frac{\omega^2}{c^2} \varepsilon(\mathbf{k}, \omega) \right] \mathbf{E}_1 = 0 \dots (11)$$

Where $\varepsilon(\mathbf{k}, \omega) = 1 - \frac{4\pi}{i\omega} \|\sigma(\mathbf{k}, \omega)\|$ is dielectric tensor.

The Maxwellian distribution function with loss-cone angle θ_c taken from Huang et al. (Lu et al. 2004) is written as

$$f_{so} = \frac{n_0}{M \pi^{3/2} \alpha_{\perp}^2 \alpha_{\parallel}} \exp \left[-\left(\frac{v_{\perp}}{\alpha_{\perp}}\right)^2 - \left(\frac{v_{\parallel}}{\alpha_{\parallel}}\right)^2 \right], \quad \left| \frac{v_{\perp}}{v_{\parallel}} \right| > \tan \theta_c \dots (12)$$

where normalization constant M is given as

$$M = \frac{1}{\sqrt{\frac{1 + \tan^2 \theta_c}{A_{\perp} + 1}}}$$

$$\|\varepsilon_{ij}(\mathbf{k}, \omega)\| = 1 + \sum \frac{4\pi \pi_s^2}{m_s \omega^2} \int \frac{J_q(\lambda_3) \|\mathbf{S}_{ij}\| d^3 v}{\omega - \mathbf{k}_{\parallel} \mathbf{v}_{\parallel} - (n+q)\omega_{cs} + p\nu} \dots (13)$$

The generalized dielectric tensor may be written as:

$$\begin{vmatrix} N^2 \cos^2 \theta_1 + \varepsilon_{11} & \varepsilon_{12} & N^2 \cos \theta_1 \sin \theta_1 + \varepsilon_{13} \\ \varepsilon_{21} & N^2 + \varepsilon_{22} & \varepsilon_{23} \\ N^2 \cos \theta_1 \sin \theta_1 + \varepsilon_{31} & \varepsilon_{32} & N^2 \sin^2 \theta_1 + \varepsilon_{33} \end{vmatrix} \dots (14)$$

After using the limits in above tensor $\mathbf{k}_{\perp} = k \sin \theta_1 \rightarrow 0$ and $\mathbf{k}_{\parallel} = k \cos \theta_1$, the generalized dielectric tensor becomes simplified tensor:

$$\begin{vmatrix} -N^2 + \varepsilon_{11} & \varepsilon_{12} & 0 \\ -\varepsilon_{21} & -N^2 + \varepsilon_{22} & 0 \\ 0 & 0 & \varepsilon_{33} \end{vmatrix} \dots (15)$$

For EMEC waves, it is rewritten in more convenient form:

$$-N^4 - 2\varepsilon_{11} N^2 + \varepsilon_{11}^2 + \varepsilon_{12}^2 = 0 \dots (16)$$

Neglecting the higher order terms of n, the relation becomes:

$$\varepsilon_{11} \pm \varepsilon_{12} = N^2 \dots (17)$$

Now the dispersion relation for whistler wave is obtained from above relation for $n=1, p=1$ and $J_p=1, J_q=1$

$$\frac{k^2 c^2}{\omega^2} = 1 + \frac{\omega_p^2}{\omega^2} \left[\left(1 + \frac{X_{ac}}{\alpha_{\perp}} \right) \left\{ \frac{\omega}{M k_{\parallel} \alpha_{\parallel}} Z(\xi) + A_T (1 + \xi Z(\xi)) \right\} + \tan^2 \theta_c \times \left\{ \left(\frac{1}{2} \right) + \xi^2 \left(1 + \xi Z(\xi) + \frac{X_{ac}}{\alpha_{\perp}} \xi (1 + \xi Z(\xi)) \right) \right\} \right]$$

where

$$X_{ac} = \frac{v \Gamma_x}{\omega_c^2 - v^2} \quad X_3 = \frac{\omega_r}{\omega_c} \quad X_4 = \frac{-v}{\omega_c}$$

$$k_3 = 1 - X_3 + X_4, \quad k_4 = \frac{X_3}{k_3}$$

$$\tilde{k} = \frac{k_{\parallel} \alpha_{\parallel}}{\omega_{cs}} \quad k_{\perp} = k_{\parallel}$$

The required expression for growth rate and real frequency are obtained as

$$\frac{\gamma}{\omega_c} = \frac{\frac{\sqrt{\lambda}}{M k_{\parallel}} \left[\left(1 + \frac{X_{ac}}{\alpha_{\perp}} \right) (A_T - k_4) + \left(\frac{\tan \theta_c k_3}{M k} \right)^2 - \frac{X_{ac} \tan \theta_c^2 k_3}{\alpha_{\perp} M k_{\parallel}} \right] k_3 \exp \left(- \left(\frac{k_3}{M k_{\parallel}} \right)^2 \right)}{\left(1 + \frac{X_{ac}}{\alpha_{\perp}} \right) \left\{ 1 + X_4 \frac{M^2 A_T (1 + X_4)}{2 k_3^2} - \frac{M^2 k_{\parallel}^2}{k_3} (A_T - k_4) \right\} + X'}$$

$$X' = \frac{X_{ac} \tan \theta_c^2}{2 \alpha_{\perp}} + \frac{(\delta - 1) k_3^2}{(1 - X_3)^2 (1 + X_4)}$$

$$X_3 = \frac{k_{\perp}^2}{2 \beta} \left[1 + X_4 \frac{M^2 A_T \beta \left(1 + \frac{X_{ac}}{\alpha_{\perp}} \right)}{(1 + X_4)^2} + \frac{X_{ac} \tan \theta_c^2 M}{2 \alpha_{\perp} k_{\parallel} (1 + X_4)} \right]$$

Where $\beta = \frac{k_{\perp} T_{\parallel} n_0 \mu_0}{B_0^2}$ and $\delta = 1 + \frac{n_c}{n_w} (1 + X_4)$

Results And Discussion:-

Following plasma parameters have been adopted for the calculation of the growth rate for the loss-cone driven whistler instability in magnetosphere. Ambient magnet field $B_0 = 2 \times 10^{-7} T$, electron density $n_0 = 5 \times 10^6 m^{-3}$ and magnitude of AC electric field $E_0 = 20 mV/m$ has been considered. Literature shows that loss cone in hot plasma component (which is background plasma in our study) of magnetosphere can lead to generation of whistler waves [Huang et al. 1990]. Therefore, we have considered the model of magnetosphere with constant external magnetic field, AC electric field, thermal anisotropy and variable finite loss cone angle. Temperature anisotropy A_T is supposed to vary from 0.25 to 0.75 and loss-cone angle θ is to vary from 0° to 30° . Electron energy, $K_B T_{\parallel}$ is taken to be 5KeV, 7.5KeV and 10KeV. Also AC frequency varies from 2 KHz to 6 KHz. A cold electron beam has been injected in background plasma such that ratio of number density of cold electrons to warm electrons (n_c/n_w) remains 10.

Figure 1 shows the variation of dimensionless growth rate with respect to wave number (\tilde{k}) for various values of temperature anisotropy A_T , in the presence of magnitude of AC electric field with frequency of 2 KHz and loss-cone angle $\theta = 10^\circ$. For $A_T = 0.25$, $\gamma/\omega_c = 0.0089$, for $A_T = 0.5$, $\gamma/\omega_c = 0.0126$ and for $A_T = 0.75$, $\gamma/\omega_c = 0.0171$. It is observed that the growth rate increases by increasing the value temperature anisotropy for $0.25 < A_T < 0.75$. It implies that temperature anisotropy behaves like a free energy source for the propagation and amplification of waves (Huang et al. 1990). It is observed that in presence of AC electric field, bandwidth increases, showing that AC field has additive effect. Therefore, minimum of electric field magnitude is enough to trigger the whistler emission and increasing the growth rate, thus increasing the power (Pandey and Kaur, 2012).

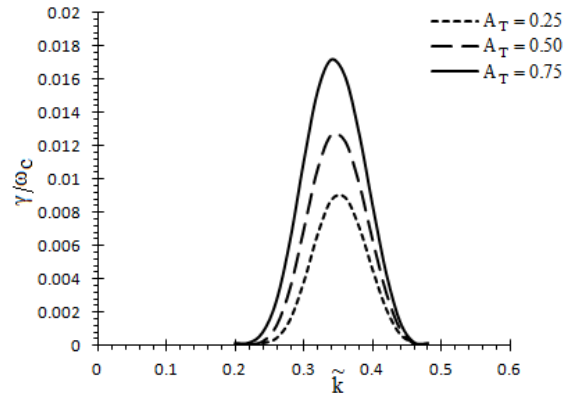


Fig.1: Variation of Growth Rate with respect to \tilde{k} for various values of Temperature Anisotropy at other fixed plasma parameters.

In **figure 2**, the variation of dimensionless growth rate with respect to wave number (\tilde{k}) for different values of loss cone angle θ , in presence of temperature anisotropy has been shown, other parameters being listed in figure caption. The growth rate is 0.0089 for $\theta = 10^\circ$ at $\tilde{k} = 0.36$, the growth rate is 0.0291 when $\theta = 20^\circ$ at $\tilde{k} = 0.40$ and growth rate is $\gamma/\omega_c = 0.0499$ for $\theta = 30^\circ$ at $\tilde{k} = 0.46$. The graph shows that growth rate increases with increasing the value of loss cone angle and bandwidth also shifts for higher order of loss cone angle. It implies that loss cone angle is also a free energy source to produce the instabilities and propagation of waves.

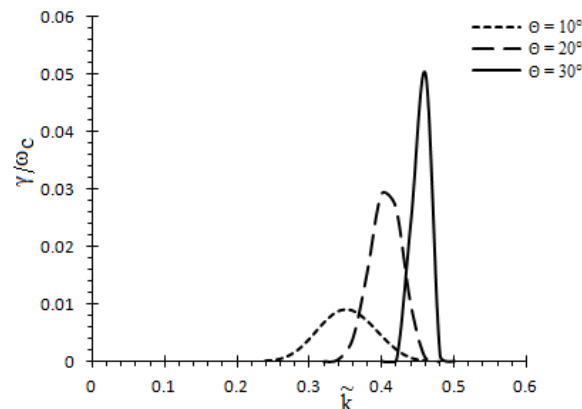


Fig.2:- Variation of Growth Rate with respect to \tilde{k} for various values of Loss-cone Angle at other fixed plasma parameters

Figure 3 shows the variation of dimensionless growth rate versus wave number (\tilde{k}) for various values of AC frequency ν , in the case when temperature anisotropy is 0.25, loss-cone angle 10° and other parameters as listed in figure caption. The growth rate for $\nu = 2\text{KHz}$ is 0.0089 at $\tilde{k} = 0.36$, the growth rate for $\nu = 4\text{KHz}$ is 0.0108 at $\tilde{k} = 0.34$ and for $\nu = 6\text{KHz}$, the growth rate is $\gamma/\omega_c = 0.0125$ at $\tilde{k} = 0.32$. The growth rate increases by increasing the AC frequency and the bandwidth is fixed. Although the effect of AC frequency is to trigger the instability, but it is seen that it also affects the growth rate marginally. Therefore, it represents the modified real frequency of waves.

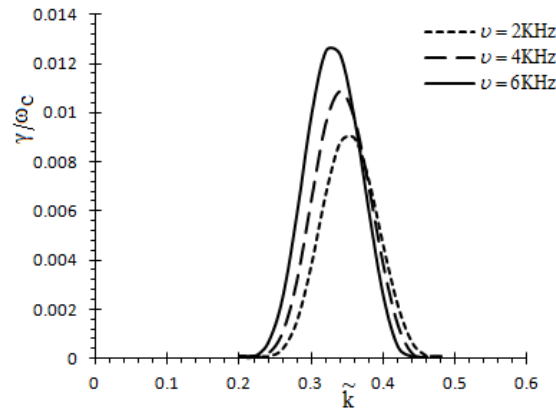


Fig.3:- Variation of Growth Rate with respect to \tilde{k} for various values of magnitude of AC Field Frequency. at other fixed plasma parameters.

Figure 4 shows the variation of dimensionless growth rate with respect to wave number (\tilde{k}) for various values of ratio of number density of cold injected electrons to warm background n_c/n_w at other plasma parameters being listed in figure caption. The number density of background warm plasma is assumed to vary to give ratios of cold and warm electrons, n_c/n_w , as 10, 20 and 30. Analysis of the figure shows that for $n_c/n_w = 10$, $\gamma/\omega_c = 0.0089$, for $n_c/n_w = 20$, $\gamma/\omega_c = 0.0047$ and for $n_c/n_w = 30$, $\gamma/\omega_c = 0.0032$ at $\tilde{k} = 0.36$. The graph shows that growth rate decreases by increasing the number density of injected cold electrons in warm background plasma of magnetosphere. The energy exchange between the electrons, the component of wave electric field, electrons and the AC field perpendicular to magnetic field are the main factors contributing to cyclotron growth or the damping of waves.

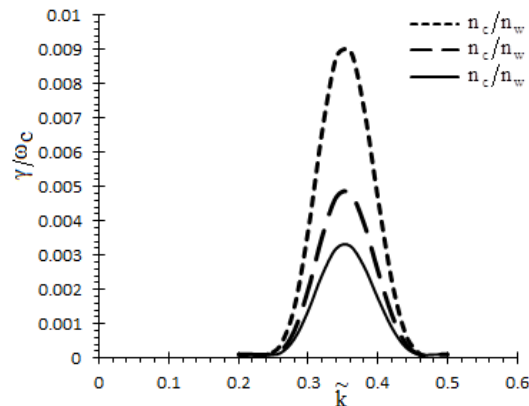


Fig. 4:- Variation of Growth Rate with respect to \tilde{k} for various values of ratio of number density of cold injected electrons to warm background n_c/n_w at other fixed plasma parameters.

Figure 5 is the graph showing the variation of dimensionless growth rate with respect to wave number (\tilde{k}) for various values of thermal energy when cold electron beam is injected. Other parameters being listed in figure caption. The magnitude of electron energy $K_B T_{||}$ has been varied. For $K_B T_{||} = 5$ KeV, growth rate is 0.0089 at $\tilde{k} = 0.36$, for $K_B T_{||} = 7.5$ KeV, growth rate is 0.0116 at $\tilde{k} = 0.4$ and for $K_B T_{||} = 10$ KeV, growth rate is 0.0137 at $\tilde{k} = 0.44$. It is seen that growth rate increases by increasing the thermal energy of background plasma and the bandwidth increases to higher order of \tilde{k} . This implies that emission is possible for extended values of \tilde{k} .

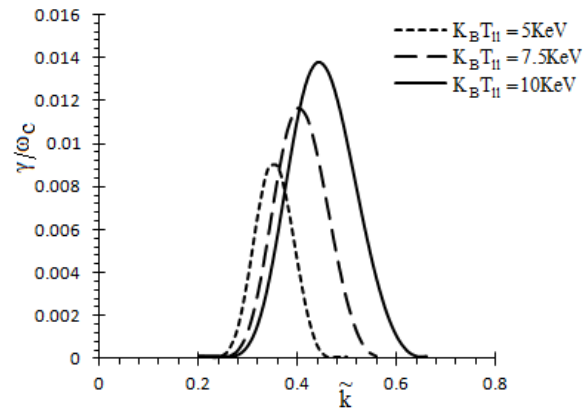


Fig. 5:- Variation of Growth Rate with respect to \tilde{k} for various values of Electron Energy $K_B T_{||}$ at other fixed plasma parameters.

In **figure 6** the variation of dimensionless growth rate versus wave number (\tilde{k}) for various values of loss cone angle for isotropic temperature has been shown and other parameters being listed in figure caption. As per graph, γ/ω_c is 0.0061 for $\theta = 10^\circ$ at $\tilde{k} = 0.36$, γ/ω_c is 0.02486 when $\theta = 20^\circ$ at $\tilde{k} = 0.42$ and γ/ω_c is 0.0491 for $\theta = 30^\circ$ at $\tilde{k} = 0.46$ in absence of temperature anisotropy. The growth rate increases and bandwidth shifts to higher value of \tilde{k} as the value of loss-cone angle increases. It is clear from figure that even if temperature anisotropy does not exit, whistler mode waves exhibit growth. Therefore, it can be said that instability has been generated due to loss cone angle.

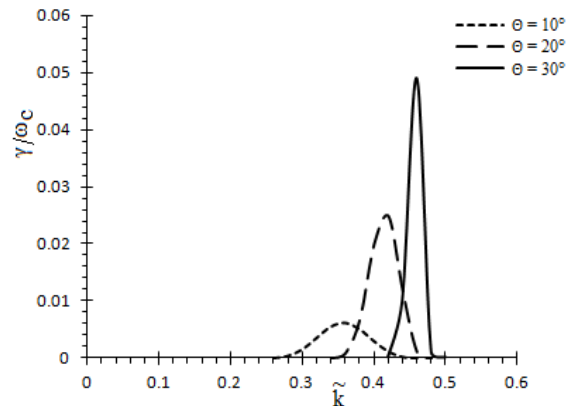


Fig.6:- Variation of Growth Rate with respect to \tilde{k} for various values of Loss-cone angle at $A_T = 0$ and other fixed plasma parameters.

Figure 7 shows the variation of dimensionless growth rate versus wave number (\tilde{k}) for various temperature anisotropy for zero loss cone angle and other parameters being listed in figure caption. For $A_T = 0.25$, $\gamma/\omega_c = 0.0037$, for $A_T = 0.5$, $\gamma/\omega_c = 0.0076$ and for $A_T = 0.75$, $\gamma/\omega_c = 0.0126$. The graph shows that growth rate increases by increasing the anisotropy for a fixed bandwidth. The increase in the growth rate is less than that in case of non-zero loss cone angle, shown in figure1.

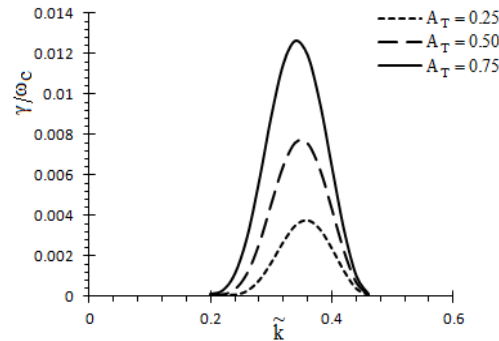


Fig.7:- Variation of Growth Rate with respect to \tilde{k} for various values of Temperature Anisotropy at Loss-cone angle $\theta = 0^\circ$ and other fixed plasma parameters.

Conclusion:-

A comprehensive study of whistler mode emissions when cold electron beam has been injected, using loss cone distribution function in the presence of perpendicular AC electric field has been done. By considering the kinetic approach and applying the method of characteristic solution, numerical calculations have been performed. The derived expressions of dispersion relation and growth rate are analyzed for whistler waves propagating parallel along the ambient magnetic field. The detailed study shows that the growth rate of electromagnetic whistler mode wave increases with increasing temperature anisotropy and loss cone angle. It is also concluded that even in the absence of temperature anisotropy, growth of whistler waves takes place. This shows that loss-cone angle is an important free energy source in generating whistler mode instability. Also frequency of AC electric field modifies the resonant frequency conditions of Doppler shift and show the triggering effect. The work also shows that growth rate of whistler mode waves decreases by increasing the number density of injected cold electrons in warm background plasma of magnetosphere.

References:-

1. Bret A., Dieckmann M.E., Deutsch C., 'Oblique electromagnetic instabilities for a hot relativistic beam interacting with a hot and magnetized plasma', *Physics of Plasma* 13, pp. 082109, 2006.
2. Brice N. M. and Lucas C., 'Influence of Magnetospheric Convection and Polar Wind Loss of Electrons from the Outer Radiation Belts', *J. Geophysical Res.* 76, pp. 90, 1971.
3. Gary S.P., 'What is a plasma instability?', *EOS* 7, pp. 529, 1992.
4. Gill R.D., *Plasma Physics and Nuclear Fusion Research*, Academic Press Inc., London: 503, 1981.
5. Huang L., Hawkins J.G. and Lee L.C., 'On the Generation of Pulsating Aurora by the Loss-Cone Driven Whistler Instability in the Equatorial Region', *J. Geophys. Res.* 95, pp. 3893, 1990.
6. Kumagai H., Hashimoto K., Kimura I. and Matsumoto H., 'Computer simulation of a Cerenkov Interaction between obliquely propagating whistler mode waves and an electron beam', *Phys. Fluids* 23, pp. 184, 1980.
7. Lu Q.M., Wang L.Q., Zhou Y. and Wang S., 'Electromagnetic Instabilities Excited by Electron Temperature Anisotropy', *Chin. Phys. Letter* 21, pp. 129, 2004.
8. Matsumoto H. and Omura Y., 'Cluster and channel effect phase bunchings by whistler waves in the nonuniform geomagnetic field', *J. Geophys. Res.* 86, pp. 779, 1981.
9. Omura Y. and Matsumoto H., 'Computer simulations of basic processes of coherent whistler wave-particle interactions in the magnetosphere', *J. Geophys. Res.* 87(A6), pp. 4435, 1982.
10. Pandey R.S. and Kaur R., 'Generation of Low Frequency Electromagnetic Wave by Injection of Cold Electron for Relativistic and Non-Relativistic Subtracted Bi-Maxwellian distribution with Perpendicular AC Electric Field for Magnetosphere of Uranus', *Progress in Electromagnetic Research B* 45, 337, 2012.
11. Pandey R.S. and Singh D.K., 'Study of electromagnetic ion-cyclotron instability in magneto plasma', *Progress In Electromagnetics Research M* 14, pp. 147, 2012.
12. Pandey R.S. and Singh D.K., 'Whistler mode instability with AC electric field for relativistic Subtracted bi-Maxwellian Magneto-Plasma', *Archives of Applied Science Research* 3(5), pp. 350, 2010.
13. Singh D., Singh S. and Singh R.P., 'Thermal effects on parallel resonance energy of whistler mode wave', *Pramana - J. Phys.* 66, pp. 467, 2006.
14. Zhang Y.L., Matsumoto H. and Omura Y., 'Linear and nonlinear interactions of an electron beam with oblique whistler and electrostatic waves in magnetosphere', *J. Geophys. Res.* 98, pp. 21353, 1993.